ISSN: 0067-2904

Stability and Hopf Bifurcation of a Delayed Prey-Predator System with Fear, Hunting Cooperative, and Allee Effect

Karrar Qahtan Al-Jubouri[1], Raid Kamel Naji [* 2]
[1]*Department of Production Engineering and Metallurgy, University of Technology-Iraq*
[2]*Department of Mathematics, College of Science, University of Baghdad, Baghdad, Iraq*

Received: 5/5/2023 Accepted: 22/6/2023 Published: 30/7/2024

Abstract

The effect of fear, the hunting cooperative process, and Allee's impact on the behavior of an ecological system are investigated and discussed. The impact of the delay of the prey's response to the predation risk is included. The Leslie-Gower growth is used to describe the growth of the predator population. Firstly, the solutions' existence, positivity, and boundedness within the limits of a suitable region in the parametric space for all time are studied. The stability of all equilibrium points under the surrounding environmental effects is established. Moreover, the occurrence of a Hopf bifurcation is discovered. The stability of the bifurcating periodic dynamic and their dynamical properties are studied. Finally, the obtained theoretical results are confirmed and validated utilizing numerical simulation. It is observed that the system possesses a bi-stable behavior and a Hopf bifurcation.

Keywords: Time delay, Fear, Allee effect, hunting cooperation, Leslie-Gower, Bi-stability.

الاستقرار وتشعب هوبف لنظام الفريسة–المفترس التباطئي بوجود تأثير الخوف والصيد التعاوني وتأثير آلي

كرار قحطان الجبوري[1] ، رائد كامل ناجي[*2]
[1] قسم هندسة الإنتاج والمعادن الجامعة التكنولوجية ، العراق
[2] قسم الرياضيات، كلية العلوم، جامعة بغداد، بغداد، العراق

الخلاصة

تم التحقيق ومناقشة تأثير الخوف وعملية الصيد التعاوني وتأثير آلي على سلوك نظام بيئي يتضمن التباطؤ في استجابة الفريسة لخطر الافتراس. استخدمنا نمو لزلي جاور لوصف النمو السكاني للمفترسات. اولاً، تم دراسة وجود الحل وإيجابية بالإضافة الى ايجاد قيد الحل ضمن فضاء المعلمات لكل الوقت. استقراريه جميع نقاط التوازن تحت تأثير البيئة المحيطة تم اثباتها. اضافة الى ذلك، تم اكتشاف ظهور تشعب الهوبف. تمت دراسة الاستقراريه الديناميكية الدورية المتشعبة وخصائصها الديناميكية. اخيراً، تم تأكيد النتائج النظرية التي تم الحصول عليها والتحقق من صحتها باستخدام المحاكاة العددية. كما لوحظ أن النظام يمتلك سلوكًا ثنائي الثبات وتشعب هوبف.

*Email: rknaji@gmail.com

1. Introduction

In ecology and evolutionary biology, the interaction of prey and predator has been modeled using nonlinear differential equation systems. Numerous ecologists and mathematicians have developed an interest in interactions that are directly related to population density impacts, such as predation, fear, refuge, competition, etc. throughout the past few decades, see [1-4] and the references therein. According to several experimental research, fear causes behavioral changes that physiologically tax prey species and negatively affect their capacity for reproduction and long-term survival. In fact, numerous analytical research demonstrated the destabilizing effects of the manipulative philosophy of fear on ecological demographics [5-8].

The iconic "Allee effect" is one of fear's harmful effects. Other reasons include genetic predispositions, sadness, a bad economy, and trouble finding the perfect mate [9,10]. To investigate the relationship between a species' growth and density, Allee [11] proposed in 1931 that if the population is too sparse, the population size will drop. The isometric linear function given by Bazykin [12] was used in the following formula to explain the Allee effect of prey:

$$\frac{dp}{dt} = rp\left(1 - \frac{p}{k}\right)(p - A).$$

This model is stated to have a strong Allee effect when $0 < A < k$ and a weak Allee effect when $A \leq 0$. Numerous researchers have looked at the effects of their influence on the behavior of dynamic systems in light of the physiological connection between the term Allee and the fear effect. For instance, Liyun et al [13] looked at how fear and additive Allee affected the prey-predator model's structure and found bifurcation points. The dynamic behavior of each of the one-species and two-species models was examined by Sourav [14], who discovered that the cost of fear can significantly limit per-capita growth and contribute to the creation of numerous Allee effects. The authors examined the stability of the interaction of an ecological model with a substantial Allee effect and functional Sokol-Howell predation [15].

The methods employed to kill individual prey are numerous and varied; current research has concentrated on cooperative hunting behavior displayed by some predators and how it affects the stability of the prey population. Duarte et al. [16] examined all the dynamics of cooperative hunting, its effects on the stability of a three-species food chain model, and the probability of extinction owing to a chaotic crisis. Both Alves and Hilker [17] provided a biological model that incorporated cooperative predator hunting with the Allee effect and described how to maintain the system's equilibrium in the event of a rapid collapse of the predator community. Using theoretical and numerical models of predator-prey interaction, Pal et al. [18] investigated the effects of the cooperative attack on members of the prey community and its contribution to raising anxiety among their numbers. Recent research by Pal et al. [19] examined a modified Leslie-Gower prey-predator model with the existence of fear as a result of predator cooperation during hunting. They found periodic trajectories across the Hopf bifurcation and an oscillation in system stability. The impacts of fear, shelter, collaboration, and harvesting on the dynamic behavior of autonomous and non-autonomous models were examined and analyzed by Mondal et al. [20]. But up to the time, this article was being written, no studies had been done on the phases of a delayed modified Leslie-Gower model under the combined influence of fear, cooperative attacking, and the Allee effect. The dynamics of ecosystems between stability and instability are directly impacted by temporal delays, which make systems more pragmatically and physiologically rich. Review the books [21-23] for more details.

The modified Leslie-Gower system is created in this study. It includes a variety of unique biological phenomena such as fear, the Allee effect, and hunting cooperation along with their effects on both species' inhabitants' daily lives. The mathematical architecture of the problem was represented using the delayed differential equations. This article is divided into the

following sections. The pragmatic interpretation of the system technique is prepared in section 2. The existence, positivity, and boundedness of each proposed model trajectory were shown in section 3 to be true. The system's equilibrium and response to various biological factors are covered in section 4. The stability of the delay system and the favorable circumstances for the Hopf bifurcations are covered in sections 5 and 6, respectively. Using the center manifold theorem, section 7 examines the direction and stability of the bifurcating periodic trajectories. The delayed system numerical simulation results, which confirmed the theoretical predictions, were presented in detail in section 8. A discussion and conclusions are included in the final portion.

2. Model Formulation

In order to comprehend the true dynamic behavior in the environment, and to maintain the diversity and balance of the ecosystem, this research proposes and studies a delayed ecological system that comprises a prey-predator and incorporates many actual biological elements. The following adopted hypotheses explain that fear of predators, cooperation during hunting processes, as well as the Allee effect, which arises from lack of interbreeding among individuals of the prey, are the biological components incorporated in the proposed system:

1. Both the populations are assumed to grow logistically so that the density of the prey species at time t denoted by $x(t)$ grows logistically with intrinsic growth rate r_0 and carrying capacity k_0, while the density of the predator species at time t denoted by $y(t)$ grows logistically with intrinsic growth rate r_1 and carrying capacity proportional with consumed prey and is given by k_1 in the absence of the prey.
2. The existence of the predator imposes fear with the discrete delay $\tau > 0$ in the growth of prey so that the fear function utilized $\frac{1}{1+\delta y(t-\tau)}$, where δ represents the fear rate.
3. Due to the existence of fear in the prey population, the interbreeding among individuals of the prey decreases, and hence the Allee effect is represented by $(x - m)$ multiplying by the growth rate, where $m > 0$ stands for the Allee effect constant.
4. The transmission of consumed prey to the predator is done by utilizing the Lotka-Volterra type of functional response with a search rate (attack rate) $\alpha > 0$, and since the predator population is assumed to have the capability of cooperative hunting then the functional response will be modified to $(\alpha + \beta\, y)x$, where $\beta > 0$ represents the cooperative hunting coefficient.

According to the above hypotheses, the dynamic of the described prey-predator model can be written using the following set of nonlinear first-order differential equations.

$$\begin{aligned} \frac{dx}{dt} &= \left(\frac{r_0\, x}{1+\delta\, y(t-\tau)}\right)\left(1-\frac{x}{k_0}\right)(x-m) - (\alpha+\beta\, y)\, xy = F_1(x,y), \\ \frac{dy}{dt} &= r_1\, y\left(1-\frac{y}{k_1+\sigma\,(\alpha+\beta\, y)\, x}\right) = F_2(x,y), \end{aligned} \tag{1}$$

where all parameters of the system (1) are positive and described in Table (1).

Table 1: Biological interpretation of system parameters

Parameter	Description
r_0	The growth rate of the prey population.
δ	The fear rate.
τ	The time taken by prey to respond to predation risk.
k_0	Carrying capacity of the prey population.
m	Allee effect constant.
α	The search rate of the prey by a predator.
β	A cooperative hunting coefficient.
r_1	The growth rate of the predator population.
k_1	Carrying capacity of predator in the absence of the prey.
σ	The conversion rate of prey biomass to predator biomass.

The initial conditions of the system (1) are taken as follows:

$$x(\theta) = \psi_1(\theta), y(\theta) = \psi_2(\theta), -\tau \leq \theta \leq 0, \quad (2)$$

where $\psi = (\psi_1, \psi_2)^T \in C$, such that $\psi_i(\theta) \geq 0,\ i = 1, 2$. Here, $C = C([-\tau, 0], \mathbb{R}_+^2)$ represents the Banach space of continuous functions defined by the interval $[-\tau, 0]$ into $\mathbb{R}_+^2$ with $\|\psi\| = sup_{-\tau \leq \theta \leq 0} \{|\psi_1(\theta)|, |\psi_2(\theta)|\}$. For biological mechanisms, it is assumed that $\psi_i(\theta) > 0,\ i = 1, 2$.

3. Properties of the solution

Obviously, the functions in the right-hand side of the system (1) are continuous and satisfy the local Lipschitz condition on C, then according to the fundamental theory of functional differential equations [24], the solution $(x(t),\ y(t))$ to the system (1) starting with any initial conditions satisfies (2) exists and is unique on $[0, \eta)$, where $0 < \eta \leq \infty$. Moreover, it is well known that a model's positivity and boundedness ensure that the model is properly posed biologically. In reality, the solutions' positivity proves that there is a population, and their boundedness shows how growth is naturally constrained by the availability of resources. As a result, theorem (1) is established for the positivity of the system (1), and theorem (2) is introduced for the boundedness.

Theorem 1. Every solution to the system (1) with the initial conditions (2) remains positive for all $t \geq 0$.

Proof. Let $X(t) = (x(t),\ y(t))^T \in \mathbb{R}_+^2$ be any solution to system (1) with initial conditions (2). Then system (1) can be written in the vector form as

$$\frac{dX(t)}{dt} = F(X(t), X(t-\tau)), \quad (3)$$

where

$$F(X(t), X(t-\tau)) = \begin{pmatrix} F_1(X(t), X(t-\tau)) \\ F_2 X(t), X(t-\tau) \end{pmatrix}$$

$$= \begin{pmatrix} x\left[r_0\left(1-\frac{x}{k_0}\right)(x-m)\left(\frac{1}{1+\delta\, y(t-\tau)}\right) - (\alpha+\beta\, y)\, xy\right] \\ y\left[r_1\left(1-\frac{y}{\sigma\,(\alpha+\beta\, y)\, x+k_1}\right)\right] \end{pmatrix},$$

with $X(t-\tau) = (x(t-\tau),\ y(t-\tau))^T$.

Thus, by integrating both sides of the system (3) from 0 to t, it is obtained that

$$\left.\begin{aligned} x(t) &= x(0)\, e^{\int_0^t \left[r_0\left(1-\frac{x(s)}{k_0}\right)(x(s)-m)\left(\frac{1}{1+\delta\, y(s-\tau)}\right)-(\alpha+\beta\, y(s))\, y(s)\right] ds} \\ y(t) &= y(0)\, e^{\int_0^t \left[r_1\left(1-\frac{y(s)}{\sigma\,(\alpha+\beta\, y(s))\, x(s)+k_1}\right)\right] ds} \end{aligned}\right\}.$$

Therefore, $x(t) > 0$ and $y(t) > 0$ for all $t \geq 0$. ■

Theorem 2. All solutions to the system (1) with the initial conditions (2) are uniformly bounded.

Proof. Let $\big(x(t), y(t)\big)$ be any positive solution of system (1) under the initial conditions (2).

Case I: If $x(0) \leq k_0$, then $x(t) \leq k_0$ for all $t \geq k_0$.
Assuming it is not true, then there exist t_1 and t_2 such that $x(t_1) = k_0$ and $x(t) > k_0$ for all $t \in (t_1, t_2)$. Thus,

$$x(t) = x(0) exp\left\{\int_0^t \mathcal{F}\big(x(s), y(s-\tau), y(s)\big)\, ds\right\},$$

where $\mathcal{F}\big(x(s), y(s-\tau), y(s)\big) = r_0\left(1-\frac{x(s)}{k_0}\right)(x(s)-m)\left(\frac{1}{1+\delta\, y(s-\tau)}\right) - \big(\alpha+\beta\, y(s)\big)\, y(s)$ can be written as follows:

$$\begin{aligned} x(t) &= x(0) exp\left\{\int_0^{t_1} \mathcal{F}\big(x(s), y(s-\tau), y(s)\big)\, ds + \int_{t_1}^{t_2} \mathcal{F}\big(x(s), y(s-\tau), y(s)\big)\, ds\right\} \\ &= x(t_1) exp\left\{\int_{t_1}^{t_2} \mathcal{F}\big(x(s), y(s-\tau), y(s)\big)\, ds\right\} < x(t_1), \end{aligned}$$

because $\mathcal{F}\big(x(s), y(s-\tau), y(s)\big) < 0$ for all $t \in (t_1, t_2)$ which is a contradiction. Therefore, $x(t) \leq k_0$ for all $t \geq 0$.

Case II: If $x(0) > k_0$, then $\lim\limits_{t \to \infty} sup\, x(t) \leq k_0$.
Suppose it is not true, then $x(t) > k_0$ for all $t > 0$ and $\mathcal{F}\big(x(s), y(s-\tau), y(s)\big) < 0$. Thus, we have

$$x(t) = x(0) exp\left\{\int_0^t \mathcal{F}\big(x(s), y(s-\tau), y(s)\big)\, ds\right\} < x(0)\ .$$

Hence, from cases I and II, we have

$$x(t) \leq max\{x(0), k_0\} \equiv M_1 \text{ for all } t \geq 0.$$

From, the predator equation of system (1), we have

$$\frac{dy}{dt} \leq \frac{r_1}{k_1} y(k_1 + \sigma\alpha M_1 - (1 - \sigma\beta M_1) y)$$

Hence, $\lim\limits_{t \to \infty} \sup y(t) \leq \left\{y(0), \frac{k_1+\sigma\alpha M_1}{1-\sigma\beta M_1}\right\}$.
Biologically, predators' survival and persistence are impossible without the need to hunt prey, therefore it is necessary to be $1 - \sigma\, \beta\, M_1 > 0$. ■

4. Existence of equilibrium points

An investigation of the equilibrium points of system (1) shows that system (1) has a number of nonnegative equilibrium points described as follows:

i. The vanishing equilibrium point $E_0 = (0, 0)$ always exists.
ii. The prey-free equilibrium point $E_1 = (0, k_1)$ always exists.
iii. The predator-free equilibrium point can be obtained by determining the roots of the following equation.

$$x^2 - (k_0 + m)\, x + k_0\, m = 0.$$

Clearly, this equation has two positive roots, which are given by $x_1 = k_0$ and $x_2 = m$. Hence, system (1) has two predator-free equilibrium points $E_{21} = (k_0, 0)$ and $E_{22} = (m, 0)$.
iv. Finally, the interior equilibrium point is denoted by $E^* = (x^*, y^*)$, where

$$y^* = \frac{\sigma\,\alpha\,x^* + k_1}{1 - \sigma\,\beta\,x^*}, \tag{4}$$

while x^* is the positive root of the following fifth-order polynomial equation

$$A_1x^5 + A_2x^4 + A_3x^3 + A_4x^2 + A_5x + A_6 = 0, \tag{5}$$

where

$$\begin{aligned}
A_1 &= \beta^3\sigma^3 r_0 > 0,\\
A_2 &= -3\beta^2\sigma^2 r_0 - m\beta^3\sigma^3 r_0 - \beta^3\sigma^3 k_0 r_0 < 0,\\
A_3 &= [\alpha^2\sigma^2 k_0 + \alpha\beta\sigma^2 k_0 k_1](\beta - \alpha\delta) + 3\beta\sigma r_0 + 3m\beta^2\sigma^2 r_0\\
&\quad + 3\beta^2\sigma^2 k_0 r_0 + m\beta^3\sigma^3 k_0 r_0,\\
A_4 &= -\alpha^2\sigma k_0 - 2\alpha^2\delta\sigma k_0 k_1 + \beta\sigma k_0 k_1^2(\beta - 2\alpha\delta) - r_0 - 3m\beta\sigma r_0\\
&\quad - 3\beta\sigma k_0 r_0 - 3m\beta^2\sigma^2 k_0 r_0,\\
A_5 &= -\alpha k_0 k_1 - \beta k_0 k_1^2 - \alpha\delta k_0 k_1^2 - \beta\delta k_0 k_1^3 + m r_0 + k_0 r_0 + 3m\beta\sigma k_0 r_0,\\
A_6 &= -m k_0 r_0 < 0.
\end{aligned}$$

Note that, the interior equilibrium point of the system (1) exists provided that there is a positive point (x^*, y^*) that represents the intersection of the two isoclines given in system (1). Obviously, from equation (4), $y^* > 0$ if and only if the following condition is met.

$$x^* < \frac{1}{\sigma\beta}. \tag{6}$$

However, equation (5) has at least one positive root. In fact, it has a unique positive root if and only if the following set of conditions holds.

$$\left.\begin{aligned}
&\beta + \frac{3\beta\sigma r_0 + 3m\beta^2\sigma^2 r_0 + 3\beta^2\sigma^2 k_0 r_0 + m\beta^3\sigma^3 k_0 r_0}{[\alpha^2\sigma^2 k_0 + \alpha\beta\sigma^2 k_0 k_1]} < \alpha\delta\\
&m r_0 + k_0 r_0 + 3m\beta\sigma k_0 r_0 < \alpha k_0 k_1 + \beta k_0 k_1^2 + \alpha\delta k_0 k_1^2 + \beta\delta k_0 k_1^3
\end{aligned}\right\}. \tag{7}$$

It has three or one positive root and hence there are three or one interior equilibrium point provided that one set of the following sets of conditions holds.

$$\left.\begin{aligned}
&A_3 > 0, A_4 < 0, A_5 < 0\\
&A_3 < 0, A_4 > 0, A_5 < 0\\
&A_3 < 0, A_4 < 0, A_5 > 0\\
&A_3 > 0, A_4 > 0, A_5 > 0\\
&A_3 > 0, A_4 > 0, A_5 < 0\\
&A_3 < 0, A_4 > 0, A_5 > 0
\end{aligned}\right\} \tag{8}$$

However, equation (5) has five, three, or one positive root and hence the number of interior equilibrium points will be the same as the number of roots if the following set of conditions holds.

$$A_3 > 0, A_4 < 0, A_5 > 0. \tag{9}$$

5. Stability Analysis

An investigation of the local stability of the system (1) close to the feasible equilibrium points is accomplished in this section. Let $\tilde{E} = (\tilde{x}, \tilde{y})$ be any equilibrium point of the system (1), or their equivalent vector form system (3), and let $x(t) = x_1(t) + \tilde{x}$ and $y(t) = y_1(t) + \tilde{y}$, where $X_1(t) = \big(x_1(t), y_1(t)\big)^T$ be the small perturbation vector, then the linearized system of system (1) at $\tilde{E}$ can be written as follows:

$$\frac{dX_1}{dt} = \frac{dX}{dt} = MX_1(t) + NX_1(t - \tau), \tag{10}$$

where $M = \left(\frac{\partial F}{\partial X(t)}\right)_{\tilde{E}}$ and $N = \left(\frac{\partial F}{\partial X(t-\tau)}\right)_{\tilde{E}}$. Thus the Jacobian matrix of the system (1) at $\tilde{E}$ can be written as:

$$J = M + Ne^{-\lambda\tau}, \tag{11}$$

where λ fulfills the characteristic equation:

$$\left|\lambda I - M - Ne^{-\lambda\tau}\right| = 0, \tag{12}$$

where

$$M = \begin{pmatrix} \frac{2r_0(k_0+m)\tilde{x}}{k_0(1+\delta\tilde{y})} - (\alpha + \beta\tilde{y})\,\tilde{y} - \frac{r_0 m + 3\left(\frac{r_0}{k_0}\right)\tilde{x}^2}{1+\delta\tilde{y}} & -(\alpha + 2\beta\tilde{y})\,\tilde{x} \\ \frac{r_1\,\sigma\,\tilde{y}^2\,(\alpha+\beta\tilde{y})}{[k_1+\sigma\tilde{x}(\alpha+\beta\,\tilde{y})]^2} & r_1\left[1 - \tilde{y}\frac{2k_1+\sigma\tilde{x}(2\alpha+\beta\tilde{y})}{[k_1+\sigma\tilde{x}(\alpha+\beta\,\tilde{y})]^2}\right] \end{pmatrix},$$

$$N = \begin{pmatrix} 0 & \frac{\left(r_0 m + \left(\frac{r_0}{k_0}\right)\tilde{x}^2\right)\delta\tilde{x}}{(1+\delta\tilde{y})^2} - \frac{r_0(k_0+m)\,\delta\tilde{x}^2}{k_0(1+\delta\tilde{y})^2} \\ 0 & 0 \end{pmatrix}.$$

Accordingly, the local stability analysis of the boundary equilibrium points of the system (1) can be summarized in the following theorem.

Theorem 3.
(1) The vanishing equilibrium point of system (1) is a saddle point for all $\tau \geq 0$.
(2) The prey-free equilibrium point of system (1) is unconditionally stable for all $\tau \geq 0$.
(3) Both the predator-free equilibrium points of system (1) are unstable for all $\tau \geq 0$.

Proof. **(1)** Substituting the equilibrium point $E_0 = (0, 0)$ in the equation (11) shows that

$$J(E_0) = \begin{pmatrix} -r_0 m & 0 \\ 0 & r_1 \end{pmatrix}.$$

Hence, the roots of the characteristic equation (12) will be given by:

$\lambda_{01} = -r_0 m < 0$ and $\lambda_{02} = r_1 > 0$.

Therefore, the vanishing equilibrium point of system (1) is a saddle point for all $\tau \geq 0$.
(2) Substituting the equilibrium point $E_1 = (0, k_1)$ in the equation (11) shows that

$$J(E_1) = \begin{pmatrix} -\left[\frac{r_0 m}{1+\delta k_1} + (\alpha + \beta k_1)\,k_1\right] & 0 \\ r_1\sigma(\alpha + \beta k_1) & -r_1 \end{pmatrix}.$$

Hence the roots of the characteristic equation (12) will be given by

$$\lambda_{11} = -\left[\frac{r_0 m}{1+\delta k_1} + (\alpha + \beta k_1)\,k_1\right] < 0 \text{ and } \lambda_{12} = -r_1 < 0.$$

Therefore, the prey-free equilibrium point of system (1) is unconditionally stable for all $\tau \geq 0$.
(3) Substituting the equilibrium points $E_{21} = (k_0, 0)$ and $E_{22} = (m, 0)$ in equation (11), respectively, shows that

$$J(E_{21}) = \begin{pmatrix} r_0(m - k_0) & -\alpha k_0 \\ 0 & r_1 \end{pmatrix}.$$

$$J(E_{22}) = \begin{pmatrix} r_0 m(1 - \frac{m}{k_0}) & -\alpha m \\ 0 & r_1 \end{pmatrix}.$$

Hence, the roots of the characteristic equation (12) will be given as follows:
For E_{21}: $\lambda_{211} = r_0(m - k_0)$ and $\lambda_{212} = r_1 > 0$.
For E_{22}: $\lambda_{221} = r_0 m(1 - \frac{m}{k_0})$ and $\lambda_{222} = r_1 > 0$.

Accordingly, for $m > k_0$, then $E_{21}$is an unstable node while E_{22} is a saddle point for all $\tau \geq 0$. However, for $m < k_0$, then E_{21} is a saddle point while E_{22} is unstable node for all $\tau \geq 0$. Finally, when $m = k_0$, then E_{21} and E_{22} are nonhyperbolic unstable points. ■

Now, the stability of the interior equilibrium point is denoted by $E^* = (x^*, y^*)$ is discussed in the following theorem.

Theorem 4. Suppose that system (1) has a unique interior equilibrium point. Then it is asymptotically stable for $\tau = 0$ if and only if the following conditions are met.

$$\left.\begin{array}{c} \frac{2r_0(k_0+m)x^*}{k_0(1+\delta y^*)} < (\alpha + \beta y^*)y^* + \frac{r_0 m + 3\left(\frac{r_0}{k_0}\right)x^{*2}}{(1+\delta y^*)} \\ 1 < y^* \frac{2k_1+\sigma x^*(2\alpha+\beta y^*)}{[k_1+\sigma x^*(\alpha+\beta y^*)]^2} \\ \frac{\left(r_0 m+\left(\frac{r_0}{k_0}\right)x^{*2}\right)\delta x^*}{(1+\delta y^*)^2} < \frac{r_0(k_0+m)\,\delta x^{*2}}{k_0(1+\delta y^*)^2} \end{array}\right\}. \quad (13)$$

However, there exists a positive delay value τ^* at which the interior equilibrium point becomes unstable for $\tau \geq \tau^*$ provided that in addition to the set of conditions (13) the following condition holds.

$$P_2^2 < P_3^2, \quad (14)$$

where all the new symbols are given in the proof.

Proof. According to equation (11), the Jacobian matrix of the system (1) at E^* can be written as

$$J(E^*) = \begin{pmatrix} a_{11} & a_{12} \\ a_{21} & a_{22} \end{pmatrix} + e^{-\lambda\tau}\begin{pmatrix} 0 & b_{12} \\ 0 & 0 \end{pmatrix}, \quad (15)$$

where

$$a_{11} = \frac{2r_0(k_0+m)x^*}{k_0(1+\delta y^*)} - (\alpha + \beta y^*)y^* - \frac{r_0 m + 3\left(\frac{r_0}{k_0}\right)x^{*2}}{(1+\delta y^*)},$$
$$a_{12} = -(\alpha + 2\beta y^*)x^*,$$
$$a_{21} = \frac{r_1\,\sigma\, y^{*2}\,(\alpha+\beta y^*)}{[k_1+\sigma\, x^*(\alpha+\beta y^*)]^2},$$
$$a_{22} = r_1\left[1 - y^* \frac{2k_1+\sigma x^*(2\alpha+\beta y^*)}{[k_1+\sigma x^*(\alpha+\beta y^*)]^2}\right],$$
$$b_{12} = \frac{\left(r_0 m+\left(\frac{r_0}{k_0}\right)x^{*2}\right)\delta x^*}{(1+\delta y^*)^2} - \frac{r_0(k_0+m)\,\delta x^{*2}}{k_0(1+\delta y^*)^2}.$$

Then, the characteristic equation (12) at E^* becomes:

$$\lambda^2 + P_1\,\lambda + P_2 + P_3\,e^{-\lambda\tau} = 0, \quad (16)$$

where

$$P_1 = -(a_{11} + a_{22}),$$
$$P_2 = a_{11}a_{22} - a_{12}a_{21},$$
$$P_3 = -a_{21}b_{12}.$$

The characteristic equation (16) is a transcendental equation, thus it is obvious that applying the Routh-Hurwitz criterion to it will be hard. Therefore, the following two scenarios are discussed in order to specify the sign of the real parts of the equation's (16) roots.

First: At $\tau = 0$, the equation (16) becomes

$$\lambda^2 + P_1\,\lambda + (P_2 + P_3) = 0. \quad (17)$$

Under the following requirements $P_1 > 0$ and $P_2 + P_3 > 0$, which are easily satisfied if and only if the set of conditions (13) is met, system (1) has an equilibrium E^* that is asymptotically stable and all roots of equation (17) have negative real parts according to the Routh-Hurwitz criterion.

Second: At $\tau > 0$, it is claimed that E^* is unstable for a positive delay value τ^*, then the roots of equation (16) must cross the imaginary axis [25], which means it is necessary to find pure imaginary such as $\lambda = i\vartheta$, with $\vartheta > 0$ satisfies the equation (16).

Now, substituting $\lambda = i\vartheta$ into the equation (16) yields:

$$-\vartheta^2 + P_2 + P_3\cos(\vartheta\tau) + i\,[P_1\vartheta - P_3\sin(\vartheta\tau)] = 0. \quad (18)$$

By separating the real and imaginary components of equation (18), it is obtained that:

$$\left.\begin{aligned} P_3\cos(\vartheta\tau) &= \vartheta^2 - P_2 \\ -P_3\sin(\vartheta\tau) &= -P_1\vartheta \end{aligned}\right\}. \tag{19}$$

By squaring and adding to each other the equations in (19) yields

$$\vartheta^4 + (P_1^2 - 2P_2)\vartheta^2 + (P_2^2 - P_3^2) = 0 \tag{20}$$

Substituting $\vartheta^2 = V$, then equation (20) becomes:

$$V^2 + (P_1^2 - 2P_2)\,V + (P_2^2 - P_3^2) = 0. \tag{21}$$

By Descartes' rule of signs, equation (21), and hence (20), has one positive root ϑ_0 if and only if the condition (14) is met. Thus, for $\tau \geq \tau^*$, the characteristic equation (16) has roots with positive real part and hence E^* becomes unstable. ■

According to the above theorem, E^* is asymptotically stable for all $\tau \in [\,0, \tau^*)$ and loses its stability once the eigenvalues cross the imaginary axis at $\tau = \tau^*$.

6. Hopf bifurcation Analysis

This section computes the value of τ^* before investigating the long-term behavior of the system (1) solution under conditions (13) and (14) for $\tau \geq \tau^*$. The system (1) experiences a Hopf bifurcation under conditions (13) and (14) for $\tau \geq \tau^*$, as will be proved in the following theorem.

Theorem 5. Assume that conditions (13)-(14) hold, then there exists $\tau^* > 0$ such that the equilibrium point E^* of the system (1) remains asymptotic stable for $0 < \tau < \tau^*$ and unstable for $\tau > \tau^*$, where

$$\tau^* = \min\left\{\frac{1}{\vartheta_0}\left(\arccos\left(\frac{\vartheta_0^2 - P_2}{P_3}\right) + 2n\pi\right)\right\}; n = 0,1, \ldots \tag{22}$$

Furthermore, the system (1) undergoes the Hopf bifurcation at E^* when $\tau = \tau^*$ provided that the following condition holds.

$$2P_3 < 2\vartheta_0^2 + P_1^2. \tag{23}$$

Proof. According to the theorem (4)**,** under the given conditions, there is a unique positive root, namely ϑ_0, that satisfies the equation (20) when $\tau = \tau^*$. Thus, the characteristic equation (16) has a pair of purely imaginary roots given by $\lambda(\tau^*) = \mp i\vartheta_0$. Otherwise, $\lambda(\tau) = \rho(\tau) \mp i\vartheta$, for all $\tau \in (\tau^* - \varepsilon, \tau^* + \varepsilon)$.

Now, from the equation (19) with $\vartheta = \vartheta_0$, it is obtained that

$$\tau_n^* = \frac{1}{\vartheta_0}\left(\arccos\left(\frac{\vartheta_0^2 - P_2}{P_3}\right) + 2n\pi\right), n = 0, 1, 2, \ldots \tag{24}$$

It is a function of ϑ_0, and τ^* can be selected as follows:

$$\tau^* = \min \tau_n^*,\ n = 0, 1, 2, \ldots$$

Now, since the system (1) has a pair of purely imaginary eigenvalues when $\tau = \tau^*$, then the system (1) undergoes the Hopf bifurcation if the transversality condition $\frac{d}{d\tau}[Re\,\{\lambda(\tau)\}]\Big|_{\tau = \tau^*} \neq 0$, where $Re\,\{\lambda(\tau)\} = \rho(\tau)$, is verified. So, by deriving the equation (16) with respect to τ [26], it is obtained that:

$$\left(2\lambda + P_1 - P_3\,\tau\, e^{-\lambda t}\right)\frac{d\lambda}{d\tau} = P_3\,\lambda e^{-\lambda t}.$$

Further simplification gives that:

$$\left(\frac{d\lambda}{d\tau}\right)^{-1} = \frac{2\lambda + P_1}{-\lambda\,(P^2 + P_1\lambda + P_3)} - \frac{\tau}{\lambda}.$$

Then, to verify the transversality condition, it is clear that

$$sign\left\{\frac{d}{d\tau}[Re\{\lambda(\tau)\}]\right\}_{\tau=\tau^*} = sign\left\{Re\left(\frac{d\lambda}{d\tau}\right)^{-1}\right\}_{\lambda=i\vartheta_0}$$
$$= sign\left\{Re\left(\frac{1}{\vartheta_0}\left(\frac{P_1+i2\vartheta_0}{P_1\vartheta_0+i(\vartheta_0^2-P_3)}-\frac{\tau}{i}\right)\right)\right\}$$
$$= sign\left[\frac{P_1^2+2(\vartheta_0^2-P_3)}{P_1^2\,\vartheta_0^2+(\vartheta_0^2-P_3)^2}\right] = sign\left[\frac{2\vartheta_0^2+P_1^2-2P_3}{P_3^2}\right]$$

Clearly, $\frac{d}{d\tau}[Re\{\lambda(\tau)\}]\Big|_{\tau=\tau^*} > 0$ due to condition (23). Hence, the system (1) undergoes the Hopf-bifurcation at $\tau = \tau^*$. ■

7. Direction and stability of Hopf bifurcation

Based on the center manifold and normal form theory given in [26], the direction of the Hopf bifurcation, and the stability of bifurcating periodic trajectories are discussed in the present section.

Theorem 6. The stability and direction of the bifurcating periodic solution can be specified under the following determined fixed quantities.

$$\left.\begin{aligned} C_1(0) &= \frac{i}{2\vartheta_0\tau^*}\left(g_{11}g_{20}-\left(2\,|g_{11}|^2+\frac{|g_{02}|^2}{3}\right)\right)+\frac{g_{21}}{2} \\ N_2 &= -\frac{Re\{C_1(0)\}}{Re\left\{\frac{d\lambda(\tau^*)}{d\tau}\right\}} \\ P_2 &= 2\,Re\{C_1(0)\} \\ M_2 &= -\frac{Im\{C_1(0)\}+N_2\,Im\left\{\frac{d\lambda(\tau^*)}{d\tau}\right\}}{\vartheta_0\tau^*} \end{aligned}\right\}. \quad (25)$$

Then, the physical properties of the Hopf bifurcation for system (1) around E^* at critical point $\tau = \tau^*$ are given below:

1. If $N_2 > 0$ ($N_2 < 0$), then direction of the Hopf bifurcation is supercritical (subcritical) and the bifurcating periodic trajectories exist for $\tau > \tau^*$ ($\tau < \tau^*$).
2. If $P_2 < 0$ ($P_2 > 0$), then the bifurcating periodic trajectories are stable (unstable).
3. If $M_2 > 0$ ($M_2 < 0$), then the period of the bifurcating periodic trajectories increase (decrease).

Proof. Utilizing the linear transformation $u_1(t) = x(t) - x^*$, $u_2(t) = y(t) - y^*$, $\mu = \tau - \tau^*$, where $\mu \in \mathbb{R}$, and then rescaling the time delay using $t \to \frac{t}{\tau}$, the system (1) yields the following functional differential equation in $C = C([-1,0], \mathbb{R}^2)$. Obviously, the value $\mu = 0$ leads to the Hopf bifurcation point τ^* that is defined in equation (22), and the periodic trajectories of system (1) are equivalent to the trajectories of the following resulting system.

$$\frac{du(t)}{dt} = L_\mu(u_t) + f(\mu, u_t), \quad (26)$$

where $u(t) = u_t = \left(u_1(t), u_2(t)\right)^T \in \mathbb{R}^2$, and $L_\mu: C \longrightarrow \mathbb{R}^2$, and $f: \mathbb{R} \times C \longrightarrow \mathbb{R}^2$, with

$$L_\mu(\varphi) = (\tau^* + \mu)\left[M^*\begin{pmatrix}\varphi_1(0)\\ \varphi_2(0)\end{pmatrix} + N^*\begin{pmatrix}\varphi_1(-1)\\ \varphi_2(-1)\end{pmatrix}\right], \quad (27)$$

$$M^* = \begin{pmatrix} f_{100}^{(1)} & f_{010}^{(1)} \\ f_{10}^{(2)} & f_{01}^{(2)} \end{pmatrix} = \begin{pmatrix} a_{11} & a_{12} \\ a_{21} & a_{22} \end{pmatrix},$$

$$N^*\begin{pmatrix} 0 & f_{001}^{(1)} \\ 0 & 0 \end{pmatrix} = \begin{pmatrix} 0 & b_{12} \\ 0 & 0 \end{pmatrix},$$

and

$$f(\mu,\varphi)=(\tau^*+\mu)\begin{bmatrix}\sum_{i+j+k\geq 2}\frac{1}{i!j!k!}\,f_{ijk}^{(1)}\,\varphi_1^i(0)\,\varphi_2^j(0)\,\varphi_3^k(-1)\\ \sum_{i+j\geq 2}\frac{1}{i!j!}\,f_{ij}^{(2)}\,\varphi_1^i(0)\,\varphi_2^j(0)\end{bmatrix}, \tag{28}$$

with $\varphi(v)=\big(\varphi_1(v),\varphi_2(v)\big)^T\in C,\quad v\in[-1,0]$, while $f^{(1)}(\varphi_1,\varphi_2,\varphi_3)$, $f^{(2)}(\varphi_1,\varphi_2)$, $f_{ijk}^{(1)}\varphi_1^i(0)\,\varphi_2^j(0)\,\varphi_3^k(-1)$, and $f_{ij}^{(2)}\varphi_1^i(0)\,\varphi_2^j(0)$ are given as follows:

$$f^{(1)}(\varphi_1,\varphi_2,\varphi_3)=\frac{(\varphi_1+x^*)\left[-r_0m+\frac{r_0(k_0+m)}{k_0}(\varphi_1+x^*)-\frac{r_0}{k_0}(\varphi_1+x^*)^2\right]}{1+\delta\varphi_2\varphi_3+\delta y^*}\ ,$$
$$-(\varphi_1+x^*)[\alpha(\varphi_2+y^*)+\beta\varphi_2(\varphi_2+2y^*)+\beta y^{*2}]$$
$$f^{(2)}(\varphi_1,\varphi_2)=r_1(\varphi_2+y^*)\left[1-\frac{(\varphi_2+y^*)}{k_1+\sigma(\varphi_1+x^*)[\alpha+\beta(\varphi_2+y^*)]}\right],$$
$$f_{ijk}^{(1)}=\left.\frac{\partial^{i+j+k}f^{(1)}}{\partial\varphi_1^i\,\varphi_2^j\,\varphi_3^k}\right|_{(\varphi_1,\varphi_2,\varphi_3)=(0,0,-1)},$$
$$f_{jk}^{(2)}=\left.\frac{\partial^{i+j}f^{(2)}}{\partial\varphi_1^i\,\varphi_2^j}\right|_{(\varphi_1,\varphi_2)=(0,0)}.$$

Moreover, direct computation gives the following higher derivatives:

$$\left.\begin{aligned}&f_{110}^{(1)}=-(\alpha+2\beta y^*),f_{101}^{(1)}=\frac{\delta\left(3\frac{r_0}{k_0}x^{*2}-2\frac{r_0(k_0+m)}{k_0}x^*+r_0m\right)}{(1+\delta y^*)^2},f_{011}^{(1)}=0,\\ &f_{200}^{(1)}=\frac{\frac{r_0(k_0+m)}{k_0}-3\frac{r_0}{k_0}x^*}{1+\delta y^*},\ f_{020}^{(1)}=-\beta x^*,f_{002}^{(1)}=\frac{2\delta x^*\left(\frac{r_0}{k_0}x^{*2}-\frac{r_0(k_0+m)}{k_0}x^*+r_0m\right)}{(1+\delta y^*)^3},\\ &f_{11}^{(2)}=r_1\sigma y^*\left[\frac{\beta y^*\Upsilon^2+2(\alpha+\beta y^*)(1-\sigma\beta x^*y^*\Upsilon)}{\Upsilon^4}\right],f_{20}^{(2)}=-\frac{r_1y^{*2}\Upsilon\sigma(\alpha+\beta y^*)^2}{\Upsilon^4}\\ &f_{02}^{(2)}=\frac{r_1\sigma\beta x^*y^*+2r_1\sigma\beta x^*y^*\Upsilon^2-r_1\sigma\beta x^*\Upsilon^2-r_1\sigma^2\beta^2x^{*2}y^*\Upsilon}{\Upsilon^4},\Upsilon=k_1+\sigma x^*(\alpha+\beta y^*).\end{aligned}\right\} \tag{29}$$

According to the Riesz representation theorem [27], there exists a 2×2 matrix given by $\eta(v,\mu)$ whose inputs are bounded variation functions such that

$$L_\mu\varphi=\int_{-1}^{0}[d\eta(v,\mu)]\varphi(v),\ \text{for}\ \varphi\in C. \tag{30}$$

In truth, it is possible to select:

$$\eta(v,\mu)=(\tau^*+\mu)\left[\begin{pmatrix}f_{100}^{(1)} & f_{010}^{(1)}\\ f_{10}^{(2)} & f_{01}^{(2)}\end{pmatrix}\delta(v)-\begin{pmatrix}0 & f_{001}^{(1)}\\ 0 & 0\end{pmatrix}\delta(v+1)\right], \tag{31}$$

where $\delta\,(v)$ denotes the Dirac delta function and is defined as

$$\delta(v)=\begin{cases}1, & v=0\\ 0, & v\neq 0\end{cases}.$$

For $\varphi\in C^1([-1,0],\mathbb{R}^2)$, define that

$$A(\mu)\varphi(v)=\begin{cases}\frac{d\varphi(v)}{dv}; & v\in[-1,0)\\ \int_{-1}^{0}d\eta(\sigma,\mu)\,\varphi(\sigma); & v=0\end{cases}, \tag{32}$$

and

$$R(\mu)\varphi(v)=\begin{cases}0; & v\in[-1,0)\\ f(\mu,\varphi); & v=0\end{cases} \tag{33}$$

Thus, system (26) corresponds to

$$\frac{du(t)}{dt}=A(\mu)\,u_t+R(\mu)\,u_t, \tag{34}$$

where, $u_t(v)=u(t+v)$ for $v\in[-1,0]$. Furthermore, for $\psi\in C^1([0,1],(\mathbb{R}^2)^*)$, define

$$A^*\psi(s) = \begin{cases} -\frac{d\psi(s)}{ds}; & s \in (0,1] \\ \int_{-1}^{0} [d\eta^T(t,0)]\,\psi(-t); & s = 0 \end{cases}, \tag{35}$$

where η^T represents the transpose matrix η. For $\varphi \in C^1([-1,0],\mathbb{R}^2)$ and $\psi \in C^1([0,1],(\mathbb{R}^2)^*)$, in order to normalize the eigenvectors of operator A and adjoint operator A^*, the following bilinear inner product is defined below

$$\langle \psi(s), \varphi(v)\rangle = \bar{\psi}(0)\,\varphi(0) - \int_{-1}^{0}\int_{\epsilon=0}^{v} \bar{\psi}(\epsilon - v)\,d\eta(v)\,\varphi(\epsilon)\,d\epsilon, \tag{36}$$

where, $\eta(v) = \eta(v,0)$. Obviously, $A = A(0)$ and $A^* = A^*(0)$ are adjoint operators, then it is obtained that $\langle \psi, A\varphi\rangle = \langle A^*\psi, \varphi\rangle$.

Now, since the system (26) undergoes the Hopf-bifurcation near equilibrium point E^*. Then system (26) has two pure imaginary eigenvalues $\mp i\vartheta_0\tau^*$ of A, which are also eigenvalues of A^*.

Now, by a simple calculation, the eigenvectors of $A(0)$ and A^* associated with the eigenvalues $\mp i\vartheta_0\tau^*$ are computed, respectively, as follows:

$$\left.\begin{aligned} q(v) &= (1,q_1)^T e^{i\vartheta_0\tau^* v} \\ q^*(s) &= D(1,q_1^*)^T e^{-i\vartheta_0\tau^* s} \end{aligned}\right\}, \tag{37}$$

where

$$\left.\begin{aligned} q_1 &= -\frac{f_{10}^{(2)}}{f_{01}^{(2)} - i\vartheta_0} \\ q_1^* &= -\frac{\left(f_{100}^{(1)} + i\vartheta_0\right)}{f_{10}^{(2)}} \end{aligned}\right\}. \tag{38}$$

Moreover, determine the parameter value of D, such that:

$$\langle q^*(s), q(v)\rangle = 1;\ \langle q^*(s), \bar{q}(v)\rangle = 0. \tag{39}$$

According to equation (36), it is observed that:

$$\begin{aligned} \langle q^*(s), q(v)\rangle &= \bar{D}\left(1,\overline{q_1^*}\right)(1,q_1)^T - \int_{-1}^{0}\int_{\epsilon=0}^{v} \bar{D}\left(1,\overline{q_1^*}\right) e^{-i\vartheta_0\tau^*(\epsilon - v)}\, d\eta(v)(1,q_1)^T e^{i\vartheta_0\tau^*\epsilon}\, d\epsilon \\ &= \bar{D}\left(1 + q_1\,\overline{q_1^*} + \tau^*\left(q_1\, f_{001}^{(1)}\right) e^{-i\vartheta_0 t^*}\right). \end{aligned}$$

Therefore, due to (39), it is obtained that

$$\left.\begin{aligned} \bar{D} &= \left(1 + q_1\,\overline{q_1^*} + \tau^*\left(q_1\, f_{001}^{(1)}\right) e^{-i\vartheta_0 t^*}\right)^{-1} \\ D &= \left(1 + \overline{q_1}\, q_1^* + \tau^*\left(\overline{q_1}\, f_{001}^{(1)}\right) e^{i\vartheta_0 t^*}\right)^{-1} \end{aligned}\right\}. \tag{40}$$

Moreover, from the adjoint property $\langle \psi, A\varphi\rangle = \langle A^*\psi, \varphi\rangle$, it is follows that $\langle q^*(s), \bar{q}(v)\rangle = 0$.

Next, using a similar technique as in [27] , the properties of the bifurcating periodic trajectories of the system (26) can be discussed and analyzed. The coefficients g_{ij} that determine the direction and stability of the Hopf bifurcation are given below

$$\left.\begin{aligned} g_{20} &= 2\,\tau^*\,\bar{D}\left(R_1 + \overline{q_1^*}\,R_5\right) \\ g_{11} &= \tau^*\,\bar{D}\left(R_2 + \overline{q_1^*}\,R_6\right) \\ g_{02} &= 2\tau^*\,\bar{D}\left(R_3 + \overline{q_1^*}\,R_7\right) \\ g_{21} &= 2\tau^*\,\bar{D}\left(R_4 + \overline{q_1^*}\,R_8\right) \end{aligned}\right\}, \tag{41}$$

where

$$\begin{aligned} R_1 &= q_1\, f_{110}^{(1)} + \overline{q_1}\, f_{101}^{(1)}\, e^{i\vartheta_0 t^*} + \frac{1}{2}\left(f_{200}^{(1)} + q_1^2\, f_{020}^{(1)} + q_1^2\, f_{002}^{(1)}\, e^{-2i\vartheta_0 t^*}\right), \\ R_2 &= f_{200}^{(1)} + q_1\overline{q_1}\left(f_{020}^{(1)} + f_{002}^{(1)}\right) + (q_1 + \overline{q_1})\left(f_{110}^{(1)} + f_{101}^{(1)}\right), \end{aligned}$$

$$R_3 = \overline{q_1}\left(f_{110}^{(1)} + f_{101}^{(1)}\ e^{\,i\vartheta_0 t^*}\right) + \frac{1}{2}\left(f_{200}^{(1)} + \overline{q_1^2}\left(f_{020}^{(1)} + f_{002}^{(1)}\ e^{\,i\vartheta_0 t^*}\right)\right),$$
$$R_4 = \mathcal{B}_1\, f_{110}^{(1)} + \mathcal{B}_2\, f_{101}^{(1)} + \mathcal{B}_3\, f_{200}^{(1)} + \mathcal{B}_4\, f_{020}^{(1)} + \frac{1}{2}\,\mathcal{B}_5\, f_{002}^{(1)},$$
$$R_5 = q_1\, f_{11}^{(2)} + \frac{1}{2}\left(f_{20}^{(2)} + q_1^2\, f_{02}^{(2)}\right),$$
$$R_6 = f_{20}^{(2)} + q_1\overline{q_1}\ f_{02}^{(2)} + (q_1 + \overline{q_1})\, f_{11}^{(2)},$$
$$R_7 = \overline{q_1}\, f_{11}^{(2)} + \frac{1}{2}\left(f_{20}^{(2)} + \overline{q_1^2}\, f_{02}^{(2)}\right),$$
$$R_8 = \mathcal{B}_1\, f_{11}^{(2)} + \mathcal{B}_3\, f_{20}^{(2)} + \mathcal{B}_6\, f_{02}^{(2)},$$

with,

$$\mathcal{B}_1 = \frac{1}{2}\,\overline{q_1}\, W_{20}^{(1)}(0) + q_1\, W_{11}^{(1)}(0) + W_{11}^{(2)}(0) + \frac{1}{2}\ W_{20}^{(2)}(0),$$
$$\mathcal{B}_2 = \frac{1}{2}\,\overline{q_1}\, W_{20}^{(1)}(0)\, e^{\,i\vartheta_0 t^*} + q_1\, W_{11}^{(1)}(0)\, e^{-i\vartheta_0 t^*} + W_{11}^{(2)}(-1) + \frac{1}{2}\ W_{20}^{(2)}(-1),$$
$$\mathcal{B}_3 = \frac{1}{2}\ W_{20}^{(1)}(0) + W_{11}^{(1)}(0),$$
$$\mathcal{B}_4 = q_1\left(\frac{1}{2} W_{20}^{(1)}(0) + W_{11}^{(1)}(0)\right) = q_1\mathcal{B}_3,$$
$$\mathcal{B}_5 = \frac{1}{2}\left(\overline{q_1}\, W_{20}^{(2)}(-1)\, e^{\,i\vartheta_0 t^*} + q_1\, W_{11}^{(2)}(-1)\, e^{-i\vartheta_0 t^*}\right),$$
$$\mathcal{B}_6 = \overline{q_1}\, W_{20}^{(1)}(0) + 2q_1\, W_{11}^{(1)}(0).$$

Clearly, the values of g_{20}, g_{11}, and g_{02} can be determined from the above findings, while g_{21} needs to determine $W_{20}(v)$ and $W_{11}(v)$. So, performing certain arithmetic procedures and solving for $W_{20}(v)$ and $W_{11}(v)$ yields:

$$\left.\begin{aligned} W_{20}(v) &= \frac{i g_{20}}{\vartheta_0 \tau^*} q(0)\, e^{\,i\vartheta_0 t^* v} + \frac{i\,\overline{g_{11}}}{3\vartheta_0\tau^*}\,\bar{q}(0)\, e^{-i\vartheta_0 t^* v} + E_1\, e^{\,2i\vartheta_0 t^* v} \\ W_{11}(v) &= -\frac{i g_{11}}{\vartheta_0 \tau^*} q(0)\, e^{\,i\vartheta_0 t^* v} + \frac{i\,\overline{g_{02}}}{\vartheta_0\tau^*}\,\bar{q}(0)\, e^{-i\vartheta_0 t^* v} + E_2 \end{aligned}\right\}, \tag{42}$$

where, $E_i = \left(E_i^{(1)}, E_i^{(2)}\right)^T \in \mathbb{R}^2$ for $i = 1,2$ are constant vectors, which can be determined from the following equations:

$$\begin{bmatrix} 2i\vartheta_0 - f_{100}^{(1)} & -\left(f_{010}^{(1)} + f_{001}^{(1)}\ e^{\,2i\vartheta_0 t^*}\right) \\ -\ f_{10}^{(2)} & 2i\vartheta_0 - f_{01}^{(2)} \end{bmatrix} \begin{bmatrix} E_1^{(1)} \\ E_1^{(2)} \end{bmatrix} = 2\begin{bmatrix} R_1 \\ R_5 \end{bmatrix} \tag{43}$$

$$\begin{bmatrix} -f_{100}^{(1)} & -\left(f_{010}^{(1)} + f_{001}^{(1)}\right) \\ -\ f_{10}^{(2)} & -f_{01}^{(2)} \end{bmatrix} \begin{bmatrix} E_2^{(1)} \\ E_2^{(2)} \end{bmatrix} = \begin{bmatrix} R_2 \\ R_6 \end{bmatrix}. \tag{44}$$

As a result, using Cramer's rule, it is obtained that

$$E_1^{(1)} = \frac{\det(\Delta_{11})}{\det(\Delta_1)},\ E_1^{(2)} = \frac{\det(\Delta_{12})}{\det(\Delta_1)},\ E_2^{(1)} = \frac{\det(\Delta_{21})}{\det(\Delta_2)},\ E_2^{(2)} = \frac{\det(\Delta_{22})}{\det(\Delta_2)} \tag{45}$$

where

$$\Delta_1 = \begin{bmatrix} 2i\vartheta_0 - f_{100}^{(1)} & -\left(f_{010}^{(1)} + f_{001}^{(1)}\ e^{\,2i\vartheta_0 t^*}\right) \\ -\ f_{10}^{(2)} & 2i\vartheta_0 - f_{01}^{(2)} \end{bmatrix},$$
$$\Delta_{11} = \begin{bmatrix} R_1 & -\left(f_{010}^{(1)} + f_{001}^{(1)}\ e^{\,2i\vartheta_0 t^*}\right) \\ R_5 & 2i\vartheta_0 - f_{01}^{(2)} \end{bmatrix},$$
$$\Delta_{12} = \begin{bmatrix} 2i\vartheta_0 - f_{100}^{(1)} & R_1 \\ -\ f_{10}^{(2)} & R_5 \end{bmatrix},$$
$$\Delta_2 = \begin{bmatrix} -f_{100}^{(1)} & -\left(f_{010}^{(1)} + f_{001}^{(1)}\right) \\ -\ f_{10}^{(2)} & -f_{01}^{(2)} \end{bmatrix},$$

$$\Delta_{21}=\begin{bmatrix} R_2 & -\left(f_{010}^{(1)}+f_{001}^{(1)}\right) \\ R_6 & -f_{01}^{(2)} \end{bmatrix},$$

$$\Delta_{22}=\begin{bmatrix} -f_{100}^{(1)} & R_2 \\ -f_{10}^{(2)} & R_6 \end{bmatrix},$$

Therefore, it becomes easy to find the value of both $W_{20}(v)$ and $W_{11}(v)$ in equation (42) using the obtained results from equation (45). Hence, the value of g_{21} in equation (41) can be determined. Finally, utilizing the determined value of g_{ij}, the value of the fixed quantities in equation (25) is obtained, then all the properties of the bifurcating Hopf bifurcation follow and the proof is completed.

8. Numerical Simulations

In the present section, the obtained theoretical results are verified utilizing numerical simulation. The influence of time delay and all other parameters on the system's (1) dynamical behavior is studied in detail using numerical solutions of the system depending on the following hypothetical Dataset of biologically feasible parameters set. System (1) is solved numerically utilizing Matlab code with version R2021a.

$$r_0 = 4, k_0 = 15, \delta = 2, m = 1, \alpha = 0.25, \beta = 0.1$$
$$r_1 = 0.5, k_1 = 1, \sigma = 0.5, \tau = 0.1. \quad (45)$$

The numerical solution of the system (1) is determined and represented in the form of a phase portrait and their time series as shown in Figure (1) using the Dataset (45) and starting from different initial points.

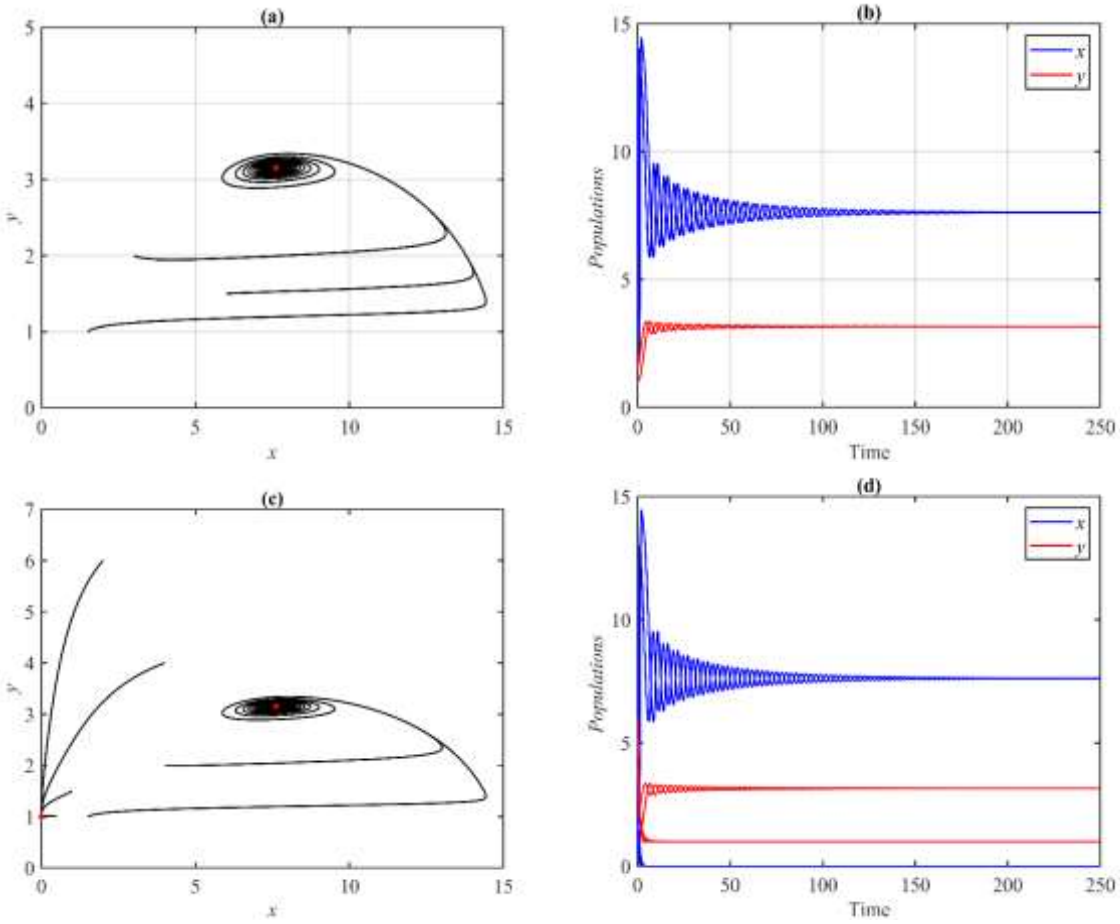

Figure 1: The trajectories of the system (1) using the dataset (45) and different initial points. (a) Approach asymptotically to $E^* = (7.61, 3.13)$. (b) The trajectories of x and y versus time.

(c) Bi-stable between $E_1 = (0,1)$ and $E^* = (7.61, 3.13)$. (d) The trajectories of x and y versus time for bistable case.

According to Figure (1), the obtained theoretical results are verified as a system (1) has unconditional stable prey-free equilibrium point. So once the initial points fall within their basin of attraction it will subsequently approach it. Moreover, since the interior equilibrium point exists and is stable the system (1) presents a bi-stable behavior. Further, the influence of r_0 on the dynamic of the system (1) is investigated in Figure (2).

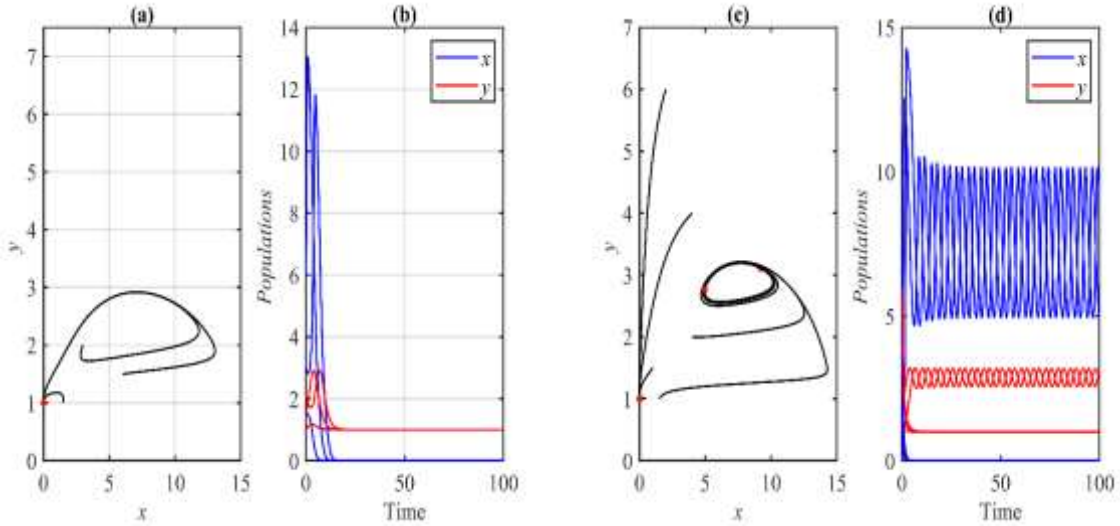

Figure 2: The trajectories of the system (1) using the dataset (45) and different initial points with different values of r_0. (a-b) The phase portrait and their time series for $r_0 = 2.5$ approaches $E_1 = (0,1)$. (c-d) The phase portrait and their time series for $r_0 = 3.5$ exhibit bi-stable between E_1 and periodic dynamics.

According to Figure (2), as the parameter r_0 increases the solution to the system (1) is transferred from the prey-free equilibrium point to the periodic in the interior of the first quadrant and then to the interior equilibrium point. The bi-stable behavior is still observed depending on the position of the initial points. Moreover, since E_1 is totally stable, the system exhibits bi-stability whenever using the initial points fall in the basin of attraction of E_1. Therefore, from now onward single initial point is used to understand the influence of the other parameters.

The influence of time delay is investigated and the obtained numerical results are shown in Figure (3).

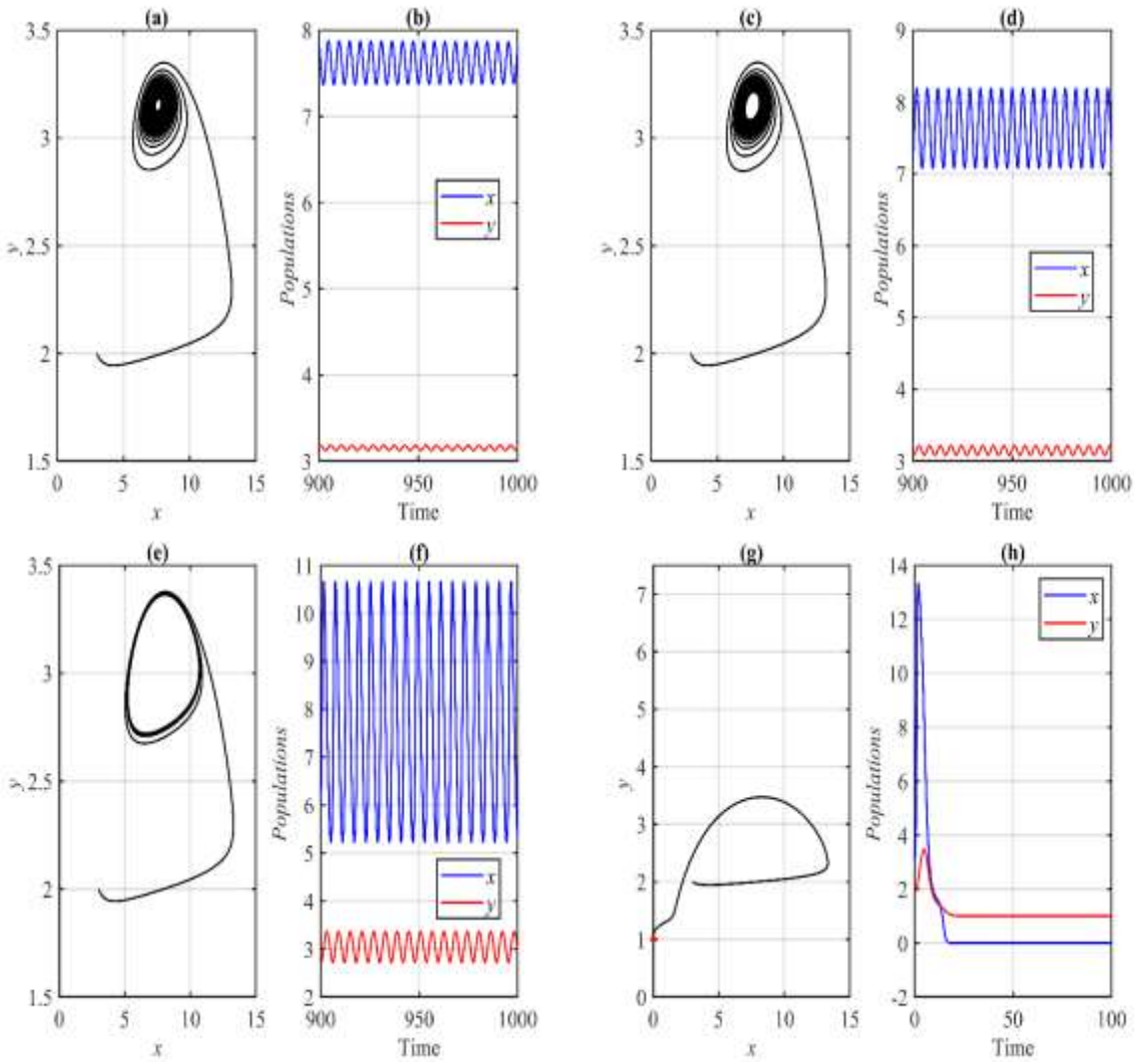

Figure 3: The trajectories of the system (1) using the dataset (45) with different values of τ. (a-b) The phase portrait and their time series for $\tau = \tau_0 = 0.188$ exhibits a Hopf bifurcation. (c-d) The phase portrait and their time series for $\tau = 0.2$ exhibit small periodic dynamics. (e-f) The phase portrait and their time series for $\tau = 0.5$ exhibit large periodic dynamics. (g-h) The phase portrait and their time series for $\tau = 1.27$ exhibit asymptotic stable E_1.

Figure (3) shows that the interior equilibrium point becomes unstable and the system (1) undergoes the Hopf bifurcation at $\tau_0 = 0.188$. Then the period starts increasing with the value of τ, and then the system loses its persistence and approaches E_1.
The influence of k_0 on the system's (1) dynamic is studied numerically and presented in Figure (4).

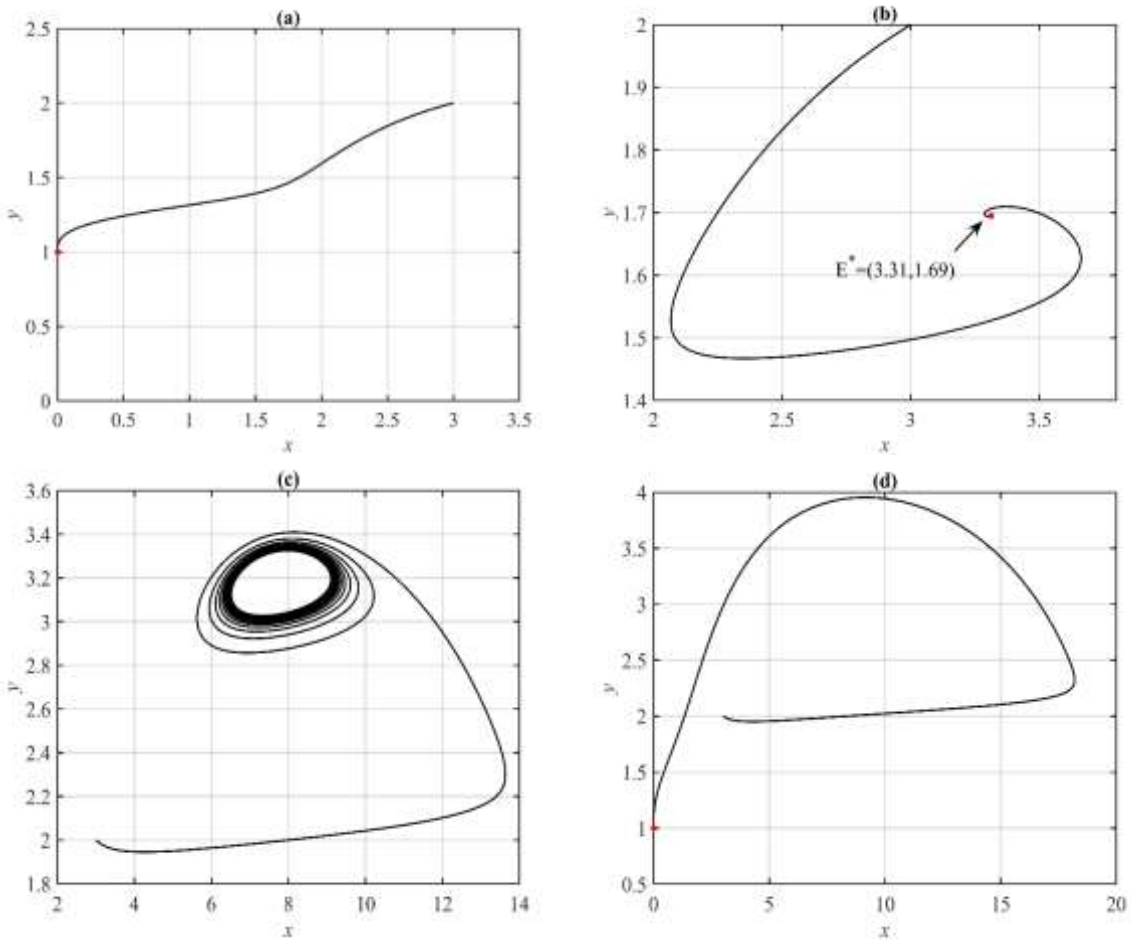

Figure 4: The trajectories of the system (1) using the dataset (45) with different values of k_0. (a) The phase portrait for $k_0 = 4.9$ approaches to E_1. (b) The phase portrait for $k_0 = 5$ approaches to E^*. (c) The phase portrait for $k_0 = 15.5$ exhibits periodic dynamics. (d) The phase portrait for $k_0 = 20$ approaches to E_1.

From Figure (4), it is observed that the behavior of the system (1), as increases k_0, transfers from E_1 to E^*, then to periodic, and finally returns back to E_1. Now, the impact of varying δ on the dynamics of the system (1) is presented in Figure (5).

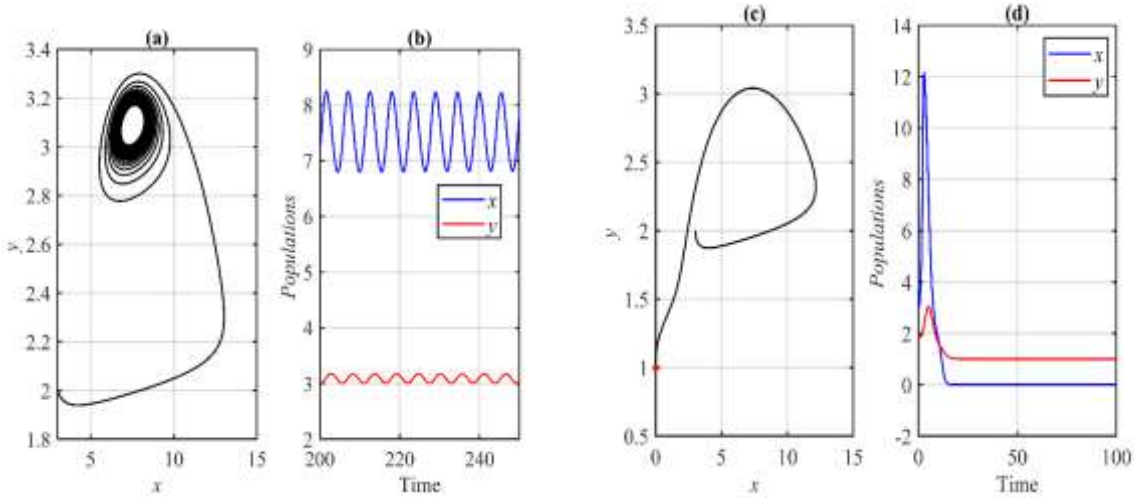

Figure 5: The trajectories of the system (1) using the dataset (45) with different values of δ. (a-b) The phase portrait and their time series for $\delta = 2.1$ exhibit periodic dynamics. (c-d) The phase portrait and their time series for $\delta = 2.9$ approaches E_1.

According to Figure (5), as increasing δ the system undergoes periodic due to the instability of E^*. Then as the parameter increases further the system approaches E_1. Now the effect of varying β on the system's (1) dynamic is studied numerically and the results are presented in Figure (6). However, the effect of varying r_1 is shown in Figure (7).

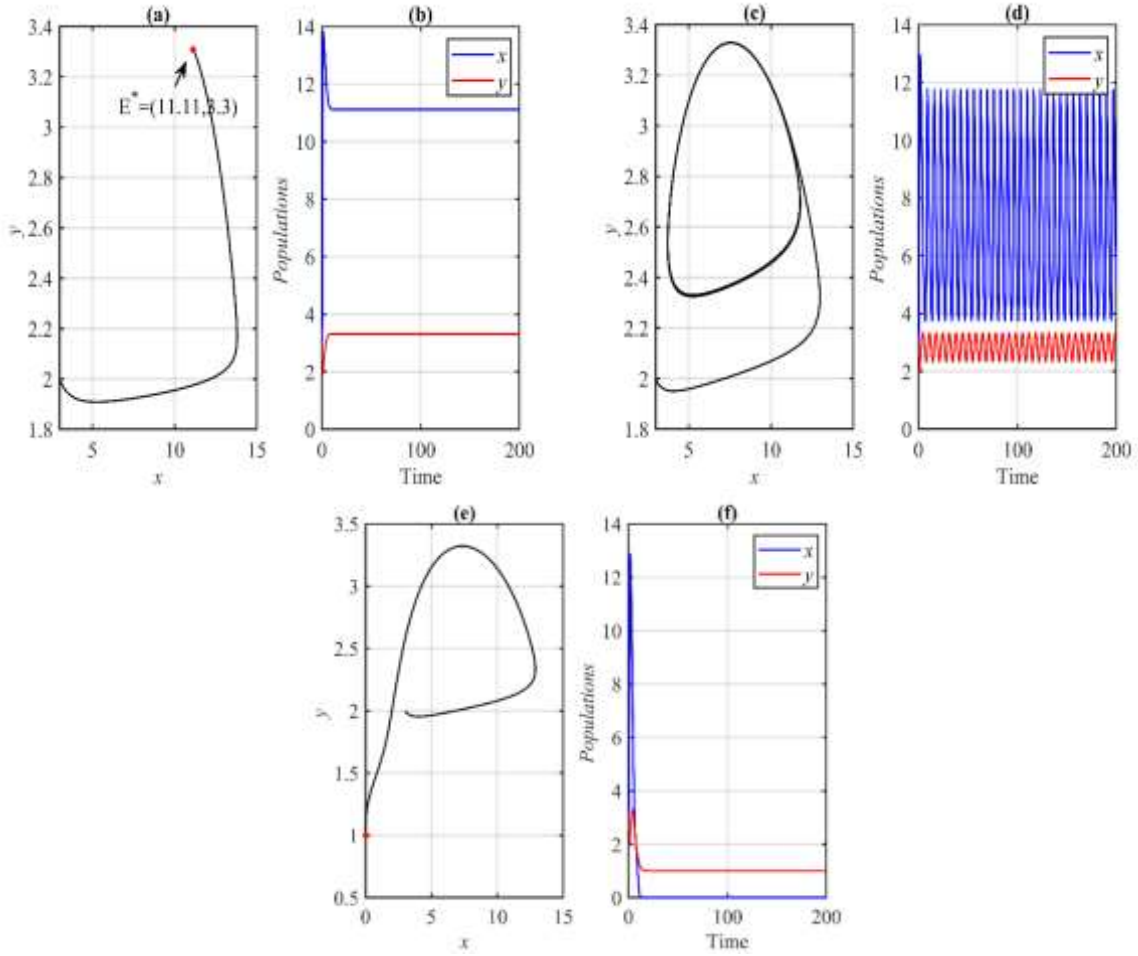

Figure 6: The trajectories of the system (1) using the dataset (45) with different values of β. (a-b) The phase portrait and their time series for $\beta = 0.05$ approaches E^*. (c-d) The phase portrait and their time series for $\beta = 0.11$ exhibit a periodic dynamics. (e-f) The phase portrait and their time series for $\beta = 0.115$ approaches E_1.

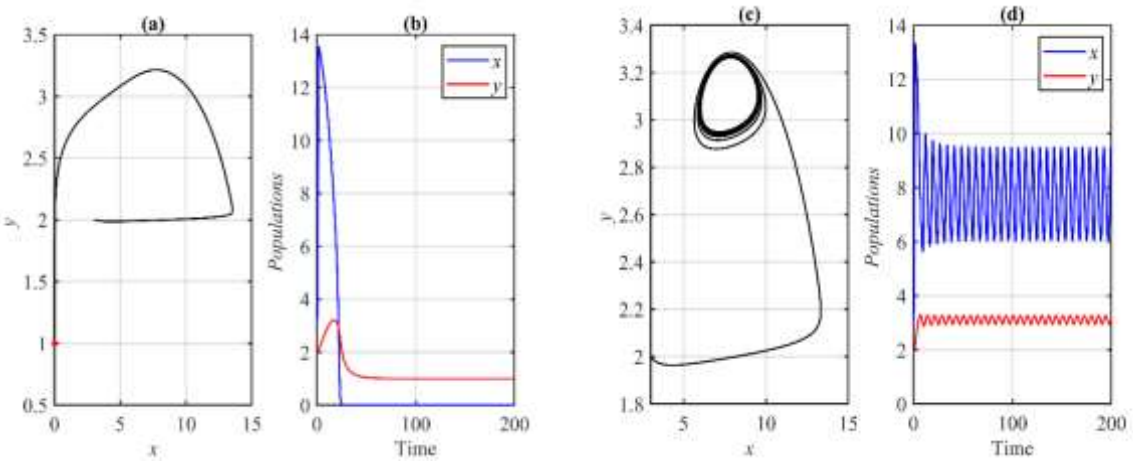

Figure 7: The trajectories of the system (1) using the dataset (45) with different values of r_1. (a-b) The phase portrait and their time series for $r_1 = 0.1$ approaches E_1. (c-d) The phase portrait and their time series for $r_1 = 0.3$ exhibit periodic dynamics.

It is observed from Figure (6) that β has a similar effect as that of δ on the system's (1) dynamic. On the other hand, Figure (7) shows that as decreases r_1 the interior equilibrium point becomes unstable and a periodic dynamic occurs. Then decreasing this parameter further makes the system approaches E_1.
Finally, the numerical simulation shows that the parameters m, α, σ, and k_1 have a similar influence on the system's (1) dynamics as that shown in δ.

9. Conclusions

A delayed prey-predator model involving fear, cooperative hunting, and the Allee effect is proposed and studied. The properties of the solution were studied. It was obtained that there exist four boundary equilibrium points. There is at least one interior equilibrium point. The stability analysis of system (1) was investigated. It is obtained that the vanishing equilibrium point of system (1) is a saddle point for all $\tau \geq 0$. While the prey-free equilibrium point of system (1) is unconditionally stable for all $\tau \geq 0$. However, Both the predator-free equilibrium points of system (1) are unstable for all $\tau \geq 0$. The interior equilibrium point is locally stable for $\tau \in [0, \tau_0)$ and unstable for $\tau_0 < \tau$. However, the system undergoes the Hopf bifurcation at τ_0. The stability and direction of the bifurcating periodic dynamics were investigated using normal form theory and center manifold theory. Numerical simulation is used to verify the obtained finding and understand the influence of parameters on the system's (1) dynamics.

According to the numerical simulation, it is observed that increasing the growth rate of the prey population has a stabilizing effect on the system's (1) dynamics. However, increasing the time prey takes to respond to predation risk (delay) has a destabilizing effect on the system's dynamic (1) up to a specific value and then the prey goes to extinction. Decreasing the carrying capacity of the prey population causes extinction in the prey population while increasing it destabilizes the interior equilibrium point first and periodic dynamics occur, then at a critical value, the system approaches a prey-free equilibrium point. Decreasing the growth rate of the predator population destabilizes the system.
It is obtained that, increasing the fear rate and a cooperative hunting coefficient destabilize the system's (1) dynamic. Similarly, as the fear rate and a combined hunting coefficient, the other parameters (Allee effect constant, the search rate of the prey by a predator, the conversion rate of prey biomass to predator biomass, and carrying capacity of predator in the absence of the prey) influence the system's (1) dynamics. Finally, since the prey-free equilibrium point is unconditionally asymptotically stable that means it has won a basin of attraction then the system

undergoes a bi-stable behavior either between the interior point and the axial point or between periodic dynamics and the axial point.

References

[1] K. Q. Al-Jubouri, S. S. Al-Bundi and . N. M. Al-Saidi, "Simulation effect of natural reserves in preserving the environmental equilibria," *International Journal of Innovative Computing, Information and Control,* vol. 16, p. 2153–2169, 2020.

[2] M. A. Stephano and I. H. Jung, "Effects of refuge prey on stability of the prey-predator model subject to immigrants: A mathematical modelling approach," *Tanzania Journal of Science,* vol. 47, pp. 1376-1391, 2021.

[3] S. D. Peacor, B. T. Barton, D. L. Kimbro, A. Sih and M. J. Sheriff, "A framework and standardized terminology to facilitate the study of predation-risk effects," *Ecology,* vol. 101, p. e03152, 2020.

[4] N. H. Fakhry and . R. K. Naji, "The dynamics of a square root prey-predator model with fear," *Iraqi Journal of Science,* vol. 61, p. 139–146, 2020.

[5] H. Qi, X. Meng, T. Hayat and A. Hobiny, "Bifurcation dynamics of a reaction-diffusion predator-prey model with fear effect in a predator-poisoned environment," *Mathematical Methods in the Applied Sciences,* vol. 45, p. 6217–6254, 2022.

[6] S. K. Sasmal and Y. Takeuchi, "Dynamics of a predator-prey system with fear and group defense," *Journal of Mathematical Analysis and Applications,* vol. 481, p. 123471, 2020.

[7] S. Pal, S. Majhi, S. Mandal and N. Pal, "Role of fear in a predator-prey model with Beddington–DeAngelis functional response," *Zeitschrift für Naturforschung A,* vol. 74, pp. 581-596, 2019.

[8] X. Dong and B. Niu, "On a diffusive predator-prey model with nonlocal fear effect," *Applied Mathematics Letters,* vol. 132, p. 108156, 2022.

[9] . F. Courchamp, L. Berec and J. Gascoigne, Allee effects in ecology and conservation, OUP Oxford, 2008.

[10] G. M. Luque, T. Giraud and F. Courchamp, "Allee effects in ants," *Journal of Animal Ecology,* vol. 82, pp. 956-965, 2013.

[11] C. G. Dittmer, Animal Aggregations: In A Study in General Sociology, Chicago, The University of Chicago Press: JSTOR, 1931.

[12] A. D. Bazykin, Nonlinear dynamics of interacting populations, World Scientific, 1998.

[13] L. Lai, Z. Zhu and F. Chen, "tability and bifurcation in a predator–prey model with the additive Allee effect and the fear effect," *Mathematics,* vol. 8, p. 1280, 2020.

[14] S. K. Sasmal, "Population dynamics with multiple Allee effects induced by fear factors–A mathematical study on prey-predator interactions," *Applied Mathematical Modelling,* vol. 64, pp. 1-14, 2018.

[15] S. Al-Momen and R. K. Naji, "The Dynamics of Sokol-Howell Prey-Predator Model Involving Strong Allee Effect," *Iraqi Journal of Science,* vol. 62, pp. 3114-3127, 2021.

[16] J. Duarte, C. Januário, N. Martins and J. Sardanyés, "Chaos and crises in a model for cooperative hunting: A symbolic dynamics approach," *Chaos: An Interdisciplinary Journal of Nonlinear Science,* vol. 19, p. 043102, 2009.

[17] M. T. Alves and F. M. Hilker, "Hunting cooperation and Allee effects in predators," *Journal of theoretical biology,* vol. 419, pp. 13-22, 2017.

[18] S. Pal, N. Pal, S. Samanta and . J. Chattopadhyay, "Effect of hunting cooperation and fear in a predator-prey model," *Ecological Complexity,* vol. 39, p. 100770, 2019.

[19] S. Pal, N. Pal, S. Samanta and J. Chattopadhyay, "Fear effect in prey and hunting cooperation among predators in a Leslie-Gower model," *Mathematical Biosciences and Engineering,* vol. 16, p. 5146, 2019.

[20] B. Mondal, S. Roy, U. Ghosh and P. K. Tiwari, "A systematic study of autonomous and nonautonomous predator–prey models for the combined effects of fear, refuge, cooperation and harvesting," *The European Physical Journal Plus,* vol. 137, p. 724, 2022.

[21] . K. Gopalsamy, Stability and oscillations in delay differential equations of population dynamics, London: Springer Science & Business Media, 1992.

[22] N. MacDonald, Biological Delay Systems: Linear Stability Theory, Cambridge University Press, 2008.

[23] . Y. Kuang, Delay Differential Equations: With Applications in Population Dynamics, Academic press, 1993.

[24] J. K. Hale, Functional differential equations, Springer US, 1971.

[25] S. Ruan and W. Wang, "Dynamical behavior of an epidemic model with a nonlinear incidence rate," *Journal of differential equations,* vol. 188, p. 135–163, 2003.

[26] B. D. Hassard , N. D. Kazarinoff, Y.-H. Wan and Y.-H. Wan, Theory and Applications of Hopf Bifurcation, Cambridge University Press, Cambridge, UK: CUP Archive, 1981.

[27] G. R. Kent, "A riesz representation theorem," *Proceedings of the American Mathematical Society,* vol. 24, p. 629–636, 1970.